J. Min. Metall. Sect. B-Metall. 53 (1) B (2017) 01 - 07

Journal of Mining and Metallurgy, Section B: Metallurgy

FIRST-PRINCIPLES GENERATED MECHANICAL PROPERTY DATABASE FOR MULTI-COMPONENT Al ALLOYS: FOCUSING ON Al-RICH CORNER

J. Wang [a,*], Y. Du [a,*], X. Tao[b], Y. Ouyang[b], L. Zhang[a], Q. Chen[c], A. Engström[c]

[a] State Key Lab of Powder Metallurgy, Central South University, Changsha, China
[b] College of Physical Science and Technology, Guangxi University, Nanning, China
[c] Thermo-Calc Software AB, Stockholm, Sweden

(Received 04 March 2016; accepted 07 November 2016)

Abstract

Systematic first-principles calculations of the single crystal elastic stiffness constants (c_{ij}'s) and the polycrystalline aggregates including bulk modulus (B), shear modulus (G), Young's modulus (E) have been performed for series binary and ternary Al compounds at 0 K. In addition, the temperature-dependent elastic properties for some technologically important phases are calculated. The c_{ij}'s are calculated by means of an efficient strain-stress method. Phonon density of states or Debye model is employed to calculate the linear thermal expansion, which is then used to calculate the temperature dependence of elastic properties. The calculated temperature-dependent elastic properties are compiled in the format of CALPHAD (CALculation of PHAse Diagram) type formula. The presently computed elastic properties for Al compounds are needed for simulation of microstructure evolution of commercial Al alloys during series of processing route.

Keywords: *Al alloys; elasticity; first-principles; CALPHAD-type database*

1. Introduction

Nowadays, computational simulations offer powerful tools to provide fundamental understanding of materials behaviors, and to support materials design that meet application requirements. The first-principles calculations are widely used to predict the thermodynamic, diffusion as well as mechanical properties of materials of interest [1-4]. Without adjustable parameters but the input of crystal structure information, the first-principles computed quantities can provide reliable "experimental data". For example, Wang et al. [2] reported systematic first-principles computed thermodynamic and elastic properties of stable Al compounds. However, so far most of the first-principles calculations are restricted to binary and/or ternary systems because of the limitation of the computational capacity. For multi-component systems, one successful modeling approach is the so-called CALPHAD (CALculation of PHAse Diagram) method [5]. The CALPHAD approach was originally developed for the modeling of thermodynamic properties by integrating experimental phase equilibria and thermochemical data via the reasonable thermodynamic models for phases. The key advantage for the CALPHAD approach is that the approach begins with the evaluation of parameters of unary, binary and ternary systems, from which the description of higher-order systems can be directly extrapolated. Recently, the CALPHAD spirit has also been applied to model other thermophysical (i.e., diffusivity, molar volume) and mechanical (i.e., elastic coefficient) properties [6-8].

Aluminum (Al) alloys with alloying elements, such as Cu, Fe, Mg, Mn, Ni, Si, and Zn, are technologically important due to their low density and good mechanical properties [9,10]. It is known that the elastic moduli of materials can be used to assess certain mechanical properties such as ductility/brittleness, hardness, strength and so on [11]. Elastic properties provide information about the interatomic bounding strength and its anisotropy, the criterion of structural stability [12,13], the measurement of lattice vibrations of acoustic modes, the correlation from an atomistic theory to a macroscopic material model [11], as well as the indications of ductility/brittleness [14], hardness [15], melting points, etc. As a consequence, the theoretical prediction of the elastic properties can provide fundamental guidance in identifying materials with desired mechanical properties.

To the best of our knowledge, there is no systematic investigation about the elastic properties of multi-component Al alloys, and thus no elastic property database is available in the literature. In view of the dearth of systematical study, the present work

Corresponding author: wangjionga@csu.edu.cn , yong-du@csu.edu.cn#*

DOI:10.2298/JMMB160304031W

aims to predict the elastic properties of single crystal elastic constants and polycrystalline aggregates, as well as temperature dependent elastic properties for binary and ternary compounds in the Al-Cu-Fe-Mg-Mn-Ni-Si-Zn system. The detail of first-principles calculations is presented in Section 2 along with brief introductions of strain-stress method herein, method to calculate temperature dependent elastic constants, and way to build mechanical properties for CALPHAD database. Section 3 shows the computed single crystal elastic constants (c_{ij}'s) together with polycrystalline aggregates including the bulk (B), shear (G), Young's (E) modulus, B/G (bulk/shear) ratio and anisotropy ratio, and temperature dependent mechanical properties for representative phases. Whenever possible, the calculations are compared with experimental data from the literature. And the summary of the present work is given in Section 4.

2. Methodology

The present first-principles calculations are performed using the projected augment wave (PAW) pseudo-potentials [16,17] as implemented in VASP (Vienna *ab initio* simulation package) [18,19], with the generalized gradient approximation (GGA) as parameterized by Perdew-Burke-Ernzerhof (PBE) [20]. All the structures are fully relaxed with respect to cell shape, volume and atomic coordinates. For consistency, the 400 eV energy cutoff is used for all the elements and compounds. The energy convergence criterion of electronic self-consistency is chosen as 10^{-6} eV/atom. The reciprocal space energy integration is performed by the Methfessel-Paxton technique [21] for structure relaxations, and for the final calculations of stresses for determining the c_{ij}'s, the linear tetrahedron method including Blöchl corrections [22] is used for the Brillouin-zone integrations. The samplings of k-points are more than 20,000 per reciprocal atom for elastic constants in terms of the Monkhorst-Pack scheme [23]. As for the estimation of the vibrational contribution to Helmholtz free energy, we adopt the phonon calculations using a supercell method [24] as implemented in the alloy theoretic automated toolkit (ATAT) [25].

The energies versus volume data points calculated from first-principles calculations are fitted by the four-parameter Birch-Murnaghan equation of state (EOS) [26]:

$$E(V) = a + bV^{-2/3} + cV^{-4/3} + dV^{-2} \quad (1)$$

where a, b, c and d are fitting parameters. In the present work, usually 10 data points in the volume range of 0.88-1.16V_0 are used for the EOS fitting of each structure. The equilibrium properties estimated from EOS include the volume (V_0), energy (E_0), bulk modulus (B_0) and its pressure derivative (B_0'). It is worth mentioning that the fitting parameters are representable by the equilibrium properties, and vice versa.

We employ the efficient strain-stress method [27,28] to calculate the elastic constants at finite temperatures. The details of the method and the parameters used in the calculations can be found elsewhere [2,27,28]. The temperature dependence of elastic constants can be obtained through first-principles calculations with the quasi-harmonic phonon approximation [4]. The Helmholtz energy of a crystal can be obtained from first-principles calculations by considering the static energy at 0 K, the lattice vibrational free energy of the lattice ions, and the thermal electronic contribution. The equilibrium volume at a given temperature, $V(T)$, can be computed through the derivative of Helmholtz energy to volume, which defines the external pressure [4]. According to Ledbetter [29], the temperature dependence of elastic constants is primarily due to the volume expansion with the increase of temperature. By calculating the elastic constants at various volumes, the temperature dependence of elastic constants can be evaluated via

$$c_{ij}(V) \xleftarrow{V(T)} c_{ij}(T) \quad (2)$$

It should be noted that the elastic constants resulting from the above equations are under isothermal conditions. In the following report, the mentioned elastic constants only refer to this kind of isothermal elastic constant. Actually, when the elastic constants are measured by resonant vibrations, the system may be viewed as adiabatic because elastic wave travels faster than heat diffuses, and the deformation due to the elastic waves is thus a constant-entropy (isentropic) process. Thus, this adiabatic or isentropic elastic constant should be different from the isothermal elastic constant. According to Liu et al. [8], the isothermal elastic constant should be smaller than the adiabatic or isentropic one for a stable phase.

Very recently, Liu et al. [8] has demonstrated one way to establish the elastic property database for Mg alloys in the form of CALPHAD formula. Different models for solution phase, stoichiometric compound and compound with certain homogeneity range have been proposed. In the present work, the first-principles calculations are devoted to the elastic constants for either stoichiometric compounds or the compounds with certain homogeneity range but only at the stoichiometric composition. And we would rather employ the following polynomial in temperature [30,31] to describe temperature-dependent elastic constant for the target phase,

$$c_{lm} = a + b \cdot T + c \cdot T^2 \quad (3)$$

where *a, b* and *c* are the coefficients to be evaluated based on the elastic constants from the first-principles calculations.

Based on the single-crystal elastic constants from the first-principles calculations shown in Eq. (9), the polycrystalline aggregate properties, such as the bulk modulus (*B*), shear modulus (*G*), and Young's modulus (*E*), can be evaluated by the Voigt's approach, which is for the upper bound based on the uniform strain and reads

$$B_V = \left(\overline{C}_{11} + 2 \cdot \overline{C}_{12}\right)/3 \quad (4)$$

$$G_V = \left(\overline{C}_{11} - \overline{C}_{12} + 3 \cdot \overline{C}_{44}\right)/5 \quad (5)$$

$$E_V = \left(9 B_V G_V\right)/\left(3B_V + G_V\right) \quad (6)$$

$$\overline{C}_{11} = \left(c_{11} + c_{22} + c_{33}\right)/3 \quad (7)$$

$$\overline{C}_{12} = \left(c_{12} + c_{13} + c_{23}\right)/3 \quad (8)$$

$$\overline{C}_{44} = \left(c_{44} + c_{55} + c_{66}\right)/3 \quad (9)$$

3. Results and discussion

Based on the method described above, we have established the CALPHAD-type elastic property database for the stable and metastable phases in the multi-component Al-Cu-Fe-Mg-Mn-Ni-Si-Zn alloys. The targeted elastic properties include the elastic constants, bulk modulus, shear modulus and Young's modulus. The presently obtained mechanical property database has been compiled into one commercial database for multi-component Al alloys (http://www.thermocalc.com). The following phases, Al_2Cu, AlCu, Al_4Cu_9, $AlCu_3$, $Al_2Cu(\theta')$, Al_3Cu_2, $Al_{13}Fe_4$, AlFe, $AlFe_3$, Al_6Fe, $AlFe_2$, Al_2Fe, $Al_{12}Mg_{17}$, $Al_{30}Mg_{23}$, Al_3Mg, Al_2Mg, $Al_{12}Mn$, Al_6Mn, $Al_{11}Mn_4$, $Al_{10}Mn_3$, Al_3Ni, Al_3Ni_2, AlNi, $AlNi_3$, $AlNi_3$, Al_9Ni_2, Al_4Ni_3, $AlNi_2$, Al_2CuMg, $Al_5Cu_6Mg_2$, $AlCu_2Mn$, Al_9FeNi, $Al_{10}Fe_3Ni$, Al_3FeSi_2, AlFeSi, $Al_3Fe_2Si_3$, $Al_{18}Mg_3Mn_2$, $Al_2Mn_2Si_3$, Al_9Mn_3Si, et al. are included in the database. In the following, the computed elastic properties for the representative phases in the Al-Ni system and two ternary compounds Al_9FeNi and $Al_{10}Fe_3Ni$ are presented.

Table 1 compares the presently calculated elastic stiffness constants (c_{ij}'s), elastic moduli (in GPa), and the anisotropy ratio at 0 K in the Al-Ni system with the experimental data and first-principles calculations available in the literature. The presently calculated elastic properties of Al_3Ni, Al_3Ni_2, AlNi, Al_3Ni_5, and $AlNi_3$ et al., are in good agreement with the literature data [32-37]. It was found that the Born stability criteria [12] of mechanical stability holds for all the phases studied herein: $\overline{C}_{44} > 0$, $\overline{C}_{11} - \left|\overline{C}_{12}\right| > 0$ and $\overline{C}_{11} + 2\overline{C}_{12} > 0$ the bulk modulus also satisfies $\overline{C}_{11} > B > \overline{C}_{12}$, implying that

Table 1. Calculated elastic stiffness constants (c_{ij}'s), elastic moduli in GPa, and Anisotropy ratio at 0 K along with the experimental and calculated data available in the literature

System	Phase	c_{11}	c_{12}	c_{13}	c_{15}	c_{22}	c_{23}	c_{25}	c_{33}	c_{35}	c_{44}	c_{46}	c_{55}	c_{66}	B*	G*	E*	B/G	A
Al-Ni	Al_3Ni	188.1	80.6	75.3		195.3	69.0		186.2		84.7		64.9	67.8	113.2	65.7	165.2	1.72	0.113
	Al_3Ni [40]	169	87	94		167	81		164		89		74	51	113				
	Al_3Ni_2	239.8	82.2	64.7					285.0		86.9			78.5	131.8	86.8	213.6	1.52	0.063
	Al_3Ni_2 [40]	226	57	33					317		93			85	119				
	AlNi	208.7	135.5								118.0				159.9	73.9	192.2	2.16	1.841
	AlNi [41]	199	137								116				158				
	AlNi [40]	170	158								101				162				
	AlNi [42]	200	140								120								
	Al_3Ni_5 [2]	248	151.4	102.9		205.6	143.9		257.7		103.5		80.5	125.7	167.5	73.6	192.6	2.28	1.433
	Al_3Ni_5 [40]	234	147	93		210	144		253		109		89	126	162				
	$AlNi_3$	241.4	149.8								128.3				180.4	84.9	220.2	2.12	1.390
	$AlNi_3$ [35]	223	148								125				173	77	202	2.25	
	$AlNi_3$ [36]	224.5	148.6								124.4				174	77	202	2.26	
	$AlNi_3$ [37]	242.2	151.8								125.4				182	83	217	2.19	
	$AlNi_3$ [40]	229	161								125				183				
	Al_9Ni_2	173	72	43	16	177	63	-7.5	200	-9.9	59	26	59		100.5	48.5	125.3	207	
	Al_4Ni_3	246	86								93				139.4	87.6	217.3	1.59	
	$AlNi_2$	240	116	95	-38				63		63				158.2	58.4	156.0	271	
Al-Fe-Ni	t_1-Al_9FeNi	200	57	41`							80		56	68	100	69	168	1.45	
	t_3-$Al_{10}Fe_3Ni$	225	93	64							92				126	78	195	1.61	

*B** = Bulk modulus, *G** = Shear modulus, *E** = Young's modulus

that these compounds are stable against elastic conformation.

Starting from c_{ij}'s, the polycrystalline aggregate properties, such as the bulk modulus (*B*), and shear modulus (*G*), can be calculated in terms of Voigt-Reuss-Hill approach and Hill approach, which gives the mean value of Voigt and Reuss. And the computed ratios of *B/G* indicate that AlNi, Al_3Ni_5, and $AlNi_3$ are ductile materials. The other phases show brittle behavior.

Elastic anisotropy ratio of a cubic crystal can be characterized by the Zener's anisotropy ratio, *A*, which represents the ratio of two shear moduli. The degree of deviation of *A* from unity 1 defines the extent of elastic anisotropy. The predicted elastic anisotropy ratios, as shown in Table 1, are in good agreement with other theoretical calculations. It is reported that the elastic anisotropy is related to the materials' resistance to microcrack [38]. The large value of *A* promotes the cross-slip pinning process due to the yielded driving force acting on screw dislocations [39]. We therefore conclude that the cubic AlNi enhances more easily and is less resistant to microcracks compared to other stable and metastable compounds.

Following the method described in Section 2, the temperature-dependent elastic constants in stable Al_3Ni, Al_3Ni_2, AlNi, Al_3Ni_5, $AlNi_3$ phases and metastable Al_4Ni_3, Al_9Ni_2, and $AlNi_2$ are calculated in the present work. According to the Al-Ni phase

Table 2. Assessed parameters ($a+b\times T+c\times T^2$) of independent elastic constants of stable and metastable compounds in the Al alloys

System	Phase	Crystal system	Independent elastic constant	Assessed parameters ($a+b\times T+c\times T^2$, $0\le T\le 1800$)
Al-Ni	Al_3Ni	Orthorhombic	C_{11}	+184.197-0.0248×T-3.854E-6×T^2
			C_{12}	+78.339-0.0165×T-1.964E-6×T^2
			C_{13}	+73.138-0.0181×T-3.811E-7×T^2
			C_{22}	+190.405-0.0306×T-4.029E-6×T^2
			C_{23}	+67.437-0.0125×T-1.791E-7×T^2
			C_{33}	+182.068-0.0285×T-5.114E-6××T^2
			C_{44}	+83.261-0.00782×T-1.901E-6×T^2
			C_{55}	+64.121-0.00551×T-8.676E-7×T^2
			C_{66}	+66.857-0.00759×T-8.572E-7×T^2
	Al_3Ni_2	Hexagonal	C_{11}	+235.466-0.0293×T-2.462E-6×T^2
			C_{12}	+79.850-0.0177×T-3.037E-7×T^2
			C_{13}	+62.900-0.0143×T-2.461E-7×T^2
			C_{33}	+279.897-0.0343×T-3.079E-6×T^2
			C_{44}	+85.828-0.00754×T-8.038E-7×T^2
	AlNi	Cubic	C_{11}	+203.473-0.03594×T-3.172E-6×T^2
			C_{12}	+131.783-0.0260×T-2.0112E-6×T^2
			C_{44}	+115.437-0.0156×T-2.393E-6×T^2
	Al_3Ni_5	Orthorhombic	C_{11}	+241.6638-0.03835×T-2.5705E-6×T^2
			C_{12}	+148.8165-0.02954×T-1.0922E-6×T^2
			C_{13}	+101.0051-0.02247×T-4.9369E-7×T^2
			C_{22}	+199.9301-0.03312×T-1.5547E-6×T^2
			C_{23}	+140.3491-0.02817×T-6.5112E-7×T^2
			C_{33}	+252.6910-0.04009×T-1.7629E-6×T^2
			C_{44}	+101.4822-0.01571×T-8.6035E-7×T^2
			C_{55}	+79.2779-0.01222×T-5.6937E-7×T^2
			C_{66}	+123.5118-0.01710×T-1.51376E-6×T^2
	$AlNi_3$	Cubic	C_{11}	+237.0176-0.0347×T-4.680E-6×T^2
			C_{12}	+146.1824-0.02825×T-2.884E-6×T^2
			C_{44}	+126.1870-0.01553×T-2.614E-6×T^2
	Al_4Ni_3	Cubic	C_{11}	+241.3104-0.03957×T-2.874E-7×T^2
			C_{12}	+83.8212-0.01954×T-5.1731E-8×T^2
			C_{44}	+92.1356-0.01195×T-1.308E-7×T^2
	$AlNi_2$	Trigonal	C_{11}	+229.6382-0.05236×T+5.2377E-7×T^2
			C_{12}	+110.4761-0.02775×T+2.6659E-7×T^2
			C_{13}	+90.7486-0.02404×T+3.6036E-7×T^2
			C_{14}	-36.3430+0.007685×T+1.4086E-7×T^2
			C_{33}	+328.0426-0.05992×T-1.4733E-6×T^2
			C_{44}	+61.4475-0.009023×T-9.5648E-7×T^2

Table 2. continued on next page

Table 2. continued from previous page

Al-Ni	Al_9Ni_2	Monoclinic	C_{11}	+169.8994-0.03494×T-3.3562E-7×T^2
			C_{12}	+70.1426-0.01775×T+4.9721E-7×T^2
			C_{13}	+42.0812-0.01998×T+1.2876E-6×T^2
			C_{15}	+42.0812-0.01998×T+1.2876E-6×T^2
			C_{22}	+173.0832-0.03519×T-7.6157E-7×T^2
			C_{23}	+61.0805-0.02311×T+2.0669E-7×T^2
			C_{25}	-7.099+0.0009627×T+5.9999E-7×T^2
			C_{33}	+196.8543-0.03369×T-2.3755E-6×T^2
			C_{35}	-9.5112+0.001286×T-1.9112E-8×T^2
			C_{44}	+57.4953-0.009376×T+1.0318E-7×T^2
			C_{46}	+2.3914-0.0007643×T+2.9752E-7×T^2
			C_{55}	+25.6002-0.008706×T+1.9078E-6×T^2
			C_{66}	+58.3008-0.008429×T-6.5622E-7×T^2
Al-Fe-Ni	Al_9FeNi	Monoclinic	C_{11}	+196.9423-0.04011×T-2.0010E-6×T^2
			C_{12}	+56.4427-0.02321×T+2.7723E-7×T^2
			C_{13}	+40.4711-0.02218×T+1.1425E-6×T^2
			C_{15}	-18.7033-0.002612×T+1.0235E-6×T^2
			C_{22}	+196.8179-0.04388×T-2.1741E-6×T^2
			C_{23}	+57.4576-0.01804×T+1.7021E-6×T^2
			C_{25}	+4.4332-0.0002332×T-1.8654E-6×T^2
			C_{33}	+196.6731-0.03762×T-1.9852E-6×T^2
			C_{35}	-11.3187+0.0007779×T-1.0379E-6×T^2
			C_{44}	+79.3927-0.01256×T-2.1218E-7×T^2
			C_{46}	-0.1943-0.0006680×T+2.7892E-10×T^2
			C_{55}	+55.2823-0.01346×T+1.1476E-6×T^2
			C_{66}	+67.9200-0.01124×T-8.3694E-7×T^2
	$Al_{10}Fe_3Ni$	Orthorhombic	C_{11}	+213.6117-0.03365×T-2.4950E-6×T^2
			C_{12}	+90.7193-0.02012×T+1.7107E-6×T^2
			C_{13}	+62.7476-0.01975×T+7.8290E-7×T^2
			C_{22}	+214.2114-0.03344×T-2.7153E-6×T^2
			C_{23}	+62.9301-0.01969×T+7.0969E-7×T^2
			C_{33}	+246.9767-0.0381×T-2.7226E-6×T^2
			C_{44}	+91.0161-0.01222×T-1.3224E-6×T^2
			C_{55}	+90.9973-0.01221×T-1.3083E-6×T^2
			C_{66}	+61.5508-0.006705×T-2.1403E-6×T^2

diagram, the Al_3Ni, Al_3Ni_5 and Al_4Ni_3 are the stoichiometric compounds, while Al_3Ni_2, AlNi and $AlNi_3$ are compounds with certain homogeneity range. Here, only the elastic constants for the stoichiometric compositions of Al_3Ni_2, AlNi and $AlNi_3$ phases are calculated. And Table 2 shows the assessed parameters (a+b×T+c×T^2) for the elastic properties of the phases in the Al-Ni system and Al-FeNi. In order to conserve space, only a stable binary phase Al_3Ni, and a metastable phase Al_4Ni_3 were taken as examples to demonstrate the accuracy of the present work in the following. More details can be found in the database for multi-component Al alloys (http://www.thermocalc.com).

Fig. 1 shows the calculated isentropic elastic constants of $AlNi_3$ phase as a function of temperature,

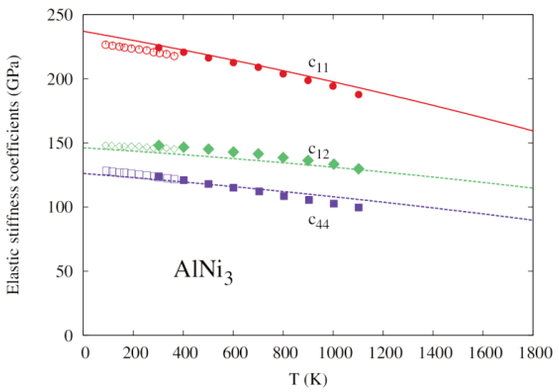

Figure 1. *Calculated temperature-dependent elastic constants of $AlNi_3$ phase in the present work along with experiment data of Tanaka and Koiwa [43] (open symbols) and Prikhodko et al [44] (solid symbols)*

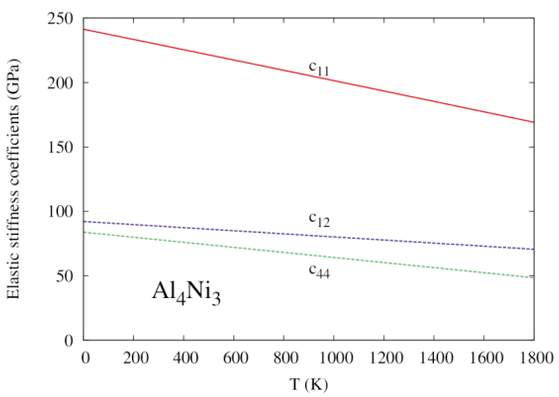

Figure 2. *Calculated temperature-dependent elastic constants of metastable Al_4Ni_3 phase in the present work*

compared with the experimental data of Tanaka and Koiwa [43] and Prikhodko et al [44]. $AlNi_3$ phase is of cubic crystal structure, and thus there are 3 independent elastic constants, i.e., c_{11}, c_{12}, and c_{44}. As can be seen in the figure, the calculated elastic constants of $AlNi_3$ phase based on the presently established mechanical property database are in good agreement with the experimental results. This figure shows the accuracy of the present work. Calculated elastic constants c_{ij} decrease with increasing temperature. In addition, the model-predicted temperature dependence of bulk modulus, shear modulus and Young's modulus of $AlNi_3$ phase can be predicted based on c_{ij} according to equations 3-9. From the equations, we know that bulk modulus decreases with increasing temperature, indicating that the hardness decreases with respect to temperature. Al_4Ni_3 is a metastable cubic phase, and the calculated temperature dependent elastic constants c_{11}, c_{12} and c_{44} are shown in Fig. 2. There are no experimental data available for this phase.

Elastic strain energy is one of a few terms for the total energy. In almost all of the previous phase field simulation for microstructure evolution, the temperature dependence of the elastic properties is not taken into account [11,45]. Such a treatment will lead to a large uncertainty for phase field simulation. This is also the case for the estimation of creep resistance. Currently, the temperature dependence of the elastic properties in the equation for the creep resistance is not considered. The presently computed elastic properties for Al compounds are needed for simulation of microstructure evolution of commercial Al alloys during series of processing route.

4. Summary

Using systematic first-principles calculations and the stress–strain method, the single-crystal elastic stiffness constants (c_{ij}'s) and polycrystalline aggregates elastic properties at 0 K for binary and ternary compounds in Al-rich corner, as well as the temperature-dependent elastic properties for some technological important phases are predicted. The predicted elastic properties are in good agreement with experimental results and theoretical data available in the literature. Elastic stiffness constants of phases are fitted by temperature related quadratic polynomial, focusing on the establishment of CALPHAD-type mechanical property database. The presently generated elastic property database for Al alloys is of interest for phase field simulation of microstructure evolution of Al alloys during series of processing route.

Acknowledgement

The financial support from the National Natural Science Foundation of China (Grant Nos. 51601228 and 51531009), and the Hunan Provincial Natural Science Foundation for Youth of China (No. 2016JJ3152) are greatly acknowledged. First-principles calculations were carried out partially on the high performance computational clusters provided by the Center of High Performance Computations at Central South University. J Wang also greatly acknowledges the Postdoctoral Science Foundation of China (Gant No. 2014M552150).

References

[1] L.J. Zhang, J. Wang, Y. Du, R.X. Hu, P. Nash, X.G. Lu, C. Jiang, Acta Mater., 57 (2009) 5324-5341.

[2] J. Wang, S.L. Shang, Y. Wang, Z.G. Mei, Y.F. Liang, Y. Du, Z.K. Liu, CALPHAD, 35 (2011) 562-573.

[3] M. Mantina, Y. Wang, L.Q. Chen, Z.K. Liu, C. Wolverton, Acta Mater., 57 (2009) 4102-4108.

[4] S.L. Shang, H. Zhang, Y. Wang, Z.K. Liu, J. Phys-Condens. Mat., 22 (2010) 375403.

[5] L. Kaufman, H. Bernstein, Computer Calculation of Phase Diagram, Academic Press Inc., New York, 1970.

[6] X.G. Lu, M. Selleby, B. Sundman, CALPHAD, 29 (2005) 49-55.

[7] J.O. Andersson, J. Ågren, J. Appl. Phys., 72 (1992) 1350-1355.

[8] Z.K. Liu, H. Zhang, S. Ganeshan, Y. Wang, S.N. Mathaudhu, Scripta Mater., 63 (2010) 686-691.

[9] G.E. Totten, M. D.S., Handbook of Aluminum, in, Marcel Dekker, New York, 2003.

[10] V.S. Zolotorevsky, N.A. Belov, M.V. Glazoff, Casting Aluminum Alloys, Elsevier, Amsterdam, 2007.

[11] L.Q. Chen, Ann. Rev. Mater. Res., 32 (2002) 113-140.

[12] M. Born, K. Huang, Dynamical Theory of Crystal Lattices, Oxford University Press, 1988.

[13] J.F. Nye, Physical Properties of Crystals: Their Representation by Tensors and Matrices, Oxford University Press, New York, 1985.

[14] S.F. Pugh, Philosophical Magazine, 45 (1954) 823-843.

[15] D.G. Clerc, H.M. Ledbetter, J. Phys. Chem. Solids, 59 (1998) 1071-1095.

[16] P.E. Blöchl, Phys. Rev. B, 50 (1994) 17953-17979.

[17] G. Kresse, D. Joubert, Phys. Rev. B, 59 (1999) 1758-1775.

[18] G. Kresse, J. Furthmuller, Phys. Rev. B, 54 (1996) 11169-11186.

[19] G. Kresse, J. Furthmuller, Comp. Mater. Sci., 6 (1996) 15-50.

[20] J.P. Perdew, K. Burke, M. Ernzerhof, Phys. Rev. Lett., 77 (1996) 3865-3868.

[21] M. Methfessel, A.T. Paxton, Phys. Rev. B, 40 (1989) 3616-3621.

[22] P.E. Blöchl, O. Jepsen, O.K. Andersen, Phys. Rev. B, 49 (1994) 16223-16233.

[23] H.J. Monkhorst, J.D. Pack, Phys. Rev. B, 13 (1976) 5188-5192.

[24] A. van de Walle, G. Ceder, Rev. Mod. Phys., 74 (2002) 11-45.

[25] A. van de Walle, CALPHAD, 33 (2009) 266-278.

[26] S.L. Shang, A. Saengdeejing, Z.G. Mei, D.E. Kim, H. Zhang, S. Ganeshan, Y. Wang, Z.K. Liu, Comp. Mater. Sci., 48 (2010) 813-826.

[27] S.L. Shang, Y. Wang, Z.K. Liu, Phys. Rev. B, 75 (2007) 024302.

[28] Y. Le Page, P. Saxe, Phys. Rev. B, 65 (2002) 104104.

[29] H. Ledbetter, Materials Science and Engineering a-Structural Materials Properties Microstructure and Processing, 442 (2006) 31-34.

[30] R. Lowrie, A.M. Gonas, J. Appl. Phys., 38 (1967) 4505-4509.

[31] O.D. Slagle, H.A. McKinstry, J. Appl. Phys., 38 (1967) 437-446.

[32] H. Zhang, S.L. Shang, Y. Wang, A. Saengdeejing, L.Q. Chen, Z.K. Liu, Acta Mater., 58 (2010) 4012-4018.

[33] D. Shi, B. Wen, R. Melnik, S. Yao, T. Lia, J. Solid State Chem., 182 (2009) 2664-2669.

[34] N. Rusović, H. Warlimont, physica status solidi (a), 44 (1977) 609-619.

[35] F.X. Kayser, C. Stassis, Phys. Status. Solidi. A, 64 (1981) 335-342.

[36] S.V. Prikhodko, J.D. Carnes, D.G. Isaak, H. Yang, A.J. Ardell, Metall. Mater. Trans. A, 30 (1999) 2403-2408.

[37] D.E. Kim, S.L. Shang, Z.K. Liu, Intermetallics, 18 (2010) 1163-1171.

[38] S. Ganeshan, S.L. Shang, Y. Wang, Z.K. Liu, J. Alloy. Compd., 498 (2010) 191-198.

[39] M.H. Yoo, Scripta Metallurgica, 20 (1986) 915-920.

[40] D.M. Shi, B. Wen, R. Melnik, S. Yao, T.J. Lia, J. Solid State Chem., 182 (2009) 2664-2669.

[41] N. Rusovic, H. Warlimont, Phys. Status. Solidi. A, 44 (1977) 609-619.

[42] Y. Mishin, M.J. Mehl, D.A. Papaconstantopoulos, Phys. Rev. B, 65 (2002) 224114.

[43] K. Tanaka, M. Koiwa, Intermetallics, 4, Supplement 1 (1996) S29-S39.

[44] S.V. Prikhodko, H. Yang, A.J. Ardell, J.D. Carnes, D.G. Isaak, Metallurgical and Materials Transactions A, 30 2403-2408.

[45] I. Steinbach, Phase-Field Model for Microstructure Evolution at the Mesoscopic Scale, in: D.R. Clarke (Ed.) Annual Review of Materials Research, Vol 43, Annual Reviews, Palo Alto, 2013, pp. 89-107.